

RESEARCH

Open Access



# Pharmacological inhibition of mTORC1 reduces neural death and damage volume after MCAO by modulating microglial reactivity

Mario Villa-González<sup>1</sup>, Marina Rubio<sup>2</sup>, Gerardo Martín-López<sup>1</sup>, Paula R. Mallavibarrena<sup>1</sup>, Laura Vallés-Saiz<sup>3</sup>, Denis Vivien<sup>2,5</sup>, Francisco Wandosell<sup>3,4\*</sup> and Maria José Pérez-Álvarez<sup>1,6\*</sup>

## Abstract

Ischemic stroke is a sudden and acute disease characterized by neuronal death, increment of reactive gliosis (reactive microglia and astrocytes), and a severe inflammatory process. Neuroinflammation is an early event after cerebral ischemia, with microglia playing a leading role. Reactive microglia involve functional and morphological changes that drive a wide variety of phenotypes. In this context, deciphering the molecular mechanisms underlying such reactive microglial is essential to devise strategies to protect neurons and maintain certain brain functions affected by early neuroinflammation after ischemia. Here, we studied the role of mammalian target of rapamycin (mTOR) activity in the microglial response using a murine model of cerebral ischemia in the acute phase. We also determined the therapeutic relevance of the pharmacological administration of rapamycin, a mTOR inhibitor, before and after ischemic injury. Our data show that rapamycin, administered before or after brain ischemia induction, reduced the volume of brain damage and neuronal loss by attenuating the microglial response. Therefore, our findings indicate that the pharmacological inhibition of mTORC1 in the acute phase of ischemia may provide an alternative strategy to reduce neuronal damage through attenuation of the associated neuroinflammation.

**Keywords** Astrocytes, Cerebral ischemia, Glia, MCAO, Microglia, mTORC1, Neuroinflammation, Neurons, Rapamycin

## Introduction

Neuroinflammation is a Central Nervous System (CNS) reactive response triggered by infection, trauma, autoimmune disorders or neurodegeneration [14]. Recent evidence suggests that neuroinflammation could aggravate damage in neurological diseases, including ischemia when not recovered in a short time period [18].

Ischemic stroke is a sudden and acute disease characterized by a severe inflammatory process [56]. It represents the second cause of death and the first cause of long-term disability worldwide [8, 9, 34]. Brain ischemia is initiated by the total or partial blockage of a cerebral artery that generates a severe reduction of oxygen and glucose supply, promoting a cellular energy failure that triggers a sequence of pathological events that induces neuronal death [6]. The different degrees of damage

\*Correspondence:

Francisco Wandosell  
fwandosell@cbm.csic.es  
Maria José Pérez-Álvarez  
mj.perez@uam.es

<sup>1</sup> Departamento de Biología (Fisiología Animal), Facultad de Ciencias, Universidad Autónoma de Madrid, Madrid, Spain

<sup>2</sup> Physiopathology and Imaging of Neurological Disorders, Normandie University, UNICAEN, UMR-S U1237, INSERM, Institut Blood and Brain @ CaenNormandie, GIP Cyceron, Caen, France

<sup>3</sup> Centro de Biología Molecular Severo Ochoa (CSIC-UAM), Madrid, Spain

<sup>4</sup> Centro de Investigaciones Biológicas en Red de Enfermedades Neurodegenerativas (CIBERNED), Madrid, Spain

<sup>5</sup> Department of Clinical Research, Caen-Normandie Hospital (CHU), Caen, France

<sup>6</sup> Instituto Universitario de Biología Molecular (IUBM-UAM), Madrid, Spain



© The Author(s) 2024. **Open Access** This article is licensed under a Creative Commons Attribution 4.0 International License, which permits use, sharing, adaptation, distribution and reproduction in any medium or format, as long as you give appropriate credit to the original author(s) and the source, provide a link to the Creative Commons licence, and indicate if changes were made. The images or other third party material in this article are included in the article's Creative Commons licence, unless indicated otherwise in a credit line to the material. If material is not included in the article's Creative Commons licence and your intended use is not permitted by statutory regulation or exceeds the permitted use, you will need to obtain permission directly from the copyright holder. To view a copy of this licence, visit <http://creativecommons.org/licenses/by/4.0/>. The Creative Commons Public Domain Dedication waiver (<http://creativecommons.org/publicdomain/zero/1.0/>) applies to the data made available in this article, unless otherwise stated in a credit line to the data.

in the ischemic area allow to distinguish two different affected regions: the infarct zone or core, and the peri-infarct region. Core is the more affected region, characterized by a drastic reduction of blood flow, whereas peri-infarct region that surrounds the core, receives a sufficient supply of nutrients to maintain certain cellular functions [7]. It has been described that neuronal damage in infarct zone is almost irreversible given that is related with high rate of necrosis. By contrast, the less damaged peri-infarct zone is potentially recoverable with an early intervention [30]. The only therapeutical approximation approved in acute phase is reperfusion, however, it does not reduce the consequent neurodegeneration [51]. Therefore, it is necessary to find alternative treatments to reduce ischemic damage and improve the beneficial effects of reperfusion.

Neuroinflammation is an early event after cerebral ischemia, being microglia a leading player. It has been described in murine models that reactive microglial response, begins 30 min after of the onset of ischemia [46]. Reactive microglial involves functional and morphological changes that drive a wide range of microglia phenotypes from pro-inflammatory to anti-inflammatory states [40]. During the acute phase of cerebral ischemia microglia release inflammatory factors that may generate a proinflammatory environment that aggravates neuronal damage [12, 54]. Therefore, understanding the molecular mechanisms underlying this early reactive microglial after ischemia could help to protect neurons and maintain brain function.

One of the main players controlling microglial functional/phenotypic changes is the PI3K/Akt/mTOR pathway [5]. mTOR is a ubiquitous serine-threonine protein kinase, highly conserved, formed by two multiprotein complexes: mTORC1 and mTORC2. Both mTOR complexes (mTORCs) coordinate a wide range of anabolic and catabolic responses, so it is considered a pivotal player in the cellular homeostasis [26, 51]. Consequently, mTOR signalling dysregulation or dysfunction significantly affect CNS integrity [20]. Several *in vivo* studies of brain ischemia have reported a decrease in mTORCs activity after ischemic damage, accompanied by neuronal death and neurological deficits [28, 32, 42]. The increase in mTORCs activity in ischemia promotes neuronal survival and diminishes ischemic damage [39, 41].

However, inhibition of mTORCs activity after or before ischemia using *in vivo* models has shown controversial results. Some reports have demonstrated detrimental effects after mTORCs inhibition while others not [2, 4, 24, 28, 55]. The involvement of mTOR along different factors such as the timing of the study, the degree of damage or the response of each cell type to ischemic injury, could explain these results. Thus, it is necessary to better

understand the role of mTORCs in all backgrounds to understand these controversial reports.

In this study, we have evaluated the role of mTOR activity after cerebral ischemia focusing on microglial response during the acute phase, by using the mTOR inhibitor rapamycin. Our data demonstrate that rapamycin administration both before and after MCAO, reduces the ischemic volume and neuronal loss and attenuates microglial response. Specifically, rapamycin reduces the levels of the pro-inflammatory microglial phenotype and promotes neuroprotection. These results suggest that the pharmacological inhibition of mTORC1, during the acute phase of ischemic stroke could be an alternative protective strategy to reduce neuronal damage through the attenuation of the neuroinflammation mediated by microglia.

## Material and methods

### Animals and treatments

Swiss mice (12 weeks old, weight 35–45 g) were housed in the Animal Facility of U1237 (GIP Cycecon) with access to food and water *ad libitum* under a 12-h light/dark cycle in a temperature-controlled environment. All care and experiments were performed following the ARRIVE guidelines ([www.nc3rs.org.uk](http://www.nc3rs.org.uk)), including blind analyses of the samples. A stock solution of rapamycin at a concentration of 20 mg/mL in ethanol was prepared. Rapamycin was diluted in 5% polyethylene glycol-400 (PEG400, Fluka) and 5% Tween<sup>®</sup>80 (Sigma-Aldrich) in phosphate-buffered saline (PBS) and administered intraperitoneally at 20 mg/kg 48 h before the induction of MCAO (MCAO + R<sub>pre</sub>) or 20 min after (MCAO + R<sub>post</sub>).

We used a total of 57 male mice, which were randomly distributed into the following experimental groups (Additional file 1: Fig. S1A): Sham + Vehicle (V), n = 10; Sham + Rapamycin (R), n = 10; MCAO + V, n = 14; MCAO + R<sub>pre</sub>, n = 12; and MCAO + R<sub>post</sub>, n = 11. We used 28 and 29 mice for western blot (WB) analysis and immunohistochemical analysis, respectively.

### Thromboembolic stroke model

Middle Cerebral Artery Occlusion (MCAO) by intravascular thrombin injection [38] was used. Animals were anesthetized with a mixture of 5% isoflurane, 1.5% O<sub>2</sub>, and 1.5% NO<sub>2</sub> and were maintained with 2–3% isoflurane during the surgical procedure according to the needs of each animal. Once the animal had been fixed in the stereotaxic frame, a craniotomy was performed on the temporal bone. Dura mater and meninges were removed until the middle cerebral artery (MCA) was isolated. A glass micropipette was then introduced into the lumen of the base of the branching MCA and 1U of purified murine  $\alpha$ -thrombin (Enzyme Research Labs) was pneumatically

introduced to induce clot formation. After 10 min, the micropipette was removed. Cerebral blood flow was monitored using a laser Doppler equipped with a fibre optic probe (Oxford Optronic) both before and up to 20 min after MCAO to verify and discard early spontaneous recanalization.

### Magnetic resonance imaging (MRI)

MRI using a Pharma Scan 7T (Bruker). Was performed on all the animals 24 h after surgery. Sequence acquisition was carried out using a Pharma Scan 7T (Bruker). Images were acquired using a TE/TR 33 ms/2500 ms multi-slice sequence. In addition, a series of T2-weighted sequences and the angiogram were obtained to monitor MCA recanalization. Lesion size was determined using Image J software. Animals that showed a lesion < 5 mm<sup>3</sup> 24 h post-MCAO were discarded.

### Western blot (WB)

Soluble protein extracts from the parietal cortex of sham and operated mice were used for WB analysis. Mice under anaesthesia were subjected to intracardiac perfusion with PBS 7.4 pH. The damaged cortex was removed and maintained at -80 °C until the subsequent analysis. Ice-cold lysis buffer [50 mM Tris 8.0 pH; 100 mM NaCl, 10 mM NaF, 5 mM EDTA, 1% Triton X-100, 1 μM okadaic acid, 2 mM sodium orthovanadate and protease inhibitors (Roche, #1,697,498)] was used to homogenize the brain samples. Homogenates were kept in ice for 15 min and centrifuged at 12,000 g for 10 min at 4 °C. Protein concentration was measured using the DC Protein Assay (Bio-Rad), following the manufacturer's protocol. Proteins were resolved on SDS-polyacrylamide gel, transferred to a 0.2 μm nitrocellulose blotting membrane (Amersham Protan), and blocked with 5% milk powder + 0.1% Tween in PBS. Membranes were incubated overnight at 4 °C with primary antibodies diluted in 5% BSA + 0.1% Tween in PBS (see Table 1). They were then washed with PBS and incubated for 1 h at room temperature with the appropriate secondary antibody: goat anti-Rabbit IgG-HRP (Southern Biotech, #4030-05) or goat anti-Mouse IgG-HRP (Southern Biotech, #1030-05) 1:5000. Immunoreactivity was detected using Clarity Western ECL substrate (Bio-Rad, #170-5061). β-Actin was used as an internal control. The relative expression levels of proteins were measured using ImageJ software (ImageJ, Fiji).

### Tissue preparation

Mice were sacrificed by intracardiac perfusion with 4% paraformaldehyde in PBS (4% PFA) under 5% isoflurane 24 h after MCAO induction. Brains were immediately removed and fixed by immersion in 4% PFA for 24 h at

**Table 1** Primary antibodies used by Western Blot analysis

Primary antibody	Host	Dilution	Trading house	Reference
Akt Total	Rabbit pAb	1:1000	Cell Signaling	9272
Akt p-Ser473	Rabbit pAb	1:1000	Cell Signaling	9271
mTOR Total	Rabbit pAb	1:1000	Cell Signaling	2972
mTOR p-Ser2448	Rabbit pAb	1:750	Cell Signaling	2971
P70S6K Total	Rabbit pAb	1:1000	Cell Signaling	9202
P70S6K p-Thr389	Rabbit pAb	1:500	Cell Signaling	9205
S6 p-Ser240/244	Rabbit pAb	1:1000	Cell Signaling	2215
GFAP	Rabbit pAb	1:1000	Cell Signaling	M0761
sTREM2	Rabbit pAb	1:1000	Alomone Labs	ANR-018
β-Actin	Mouse mAb	1:2000	Sigma-Aldrich	A5441

4 °C. They were then cryoprotected using sucrose solution and finally embedded in Tissue-Tek medium (Sakura Finetek). Brain sections were cut into 10 μm thick coronal slices from Bregma + 1 to - 2 mm [11].

### Immunohistochemistry and immunofluorescence

For immunohistochemical staining, brain sections were incubated in blocking solution (0.1% Triton X-100, 1% BSA, 1% Horse Serum in PBS) for 1 h and incubated overnight at 4 °C with the specific primary antibody: mouse anti-NeuN 1:200 (Millipore, MAB377), rabbit anti-GFAP 1:1000 (Dako, M0761) or rabbit anti-Iba-1 1:500 (Wako, 019-19741) diluted in blocking solution. Endogenous peroxidase activity was inhibited with 0.1% H<sub>2</sub>O<sub>2</sub> in PBS. After washing, samples were incubated with the appropriate secondary antibody using the ABC kit (Vectastain® ABC, Vector Laboratories, USA), following the manufacturer's instructions. Secondary antibodies were visualized using diaminobenzidine (DAB). Coverslips were mounted with Depex (Panreac) and images were captured using an Olympus BX51 microscope with an Olympus camera DP-70 (Olympus).

For immunofluorescence staining, samples were pre-treated for 30 min with 0.1 M Glycine 8.5 pH. They were then blocked for 1 h and incubated overnight at 4 °C with guinea pig anti-Iba-1 1:750 (LabClinics, #HS-234004), rabbit anti-S6 p-Ser240/244 1:200 (Cell Signaling, #2215) or rabbit anti-sTREM2 1:300 (Alomone Labs, #ANR018) diluted in blocking solution. The following day, samples were washed in PBS and incubated with the appropriate secondary antibody: anti-rabbit Alexa 488 and anti-guinea pig Alexa 555, both 1:1000 (AlexaFluor, Thermo-Fisher). After washing, nuclei were stained with DAPI 1:5000 (Calbiochem) for 5 min. Sections were mounted with Fluoromount-G (Southern Biotechnology Associates).

Images were captured using a confocal laser scanning microscope LSM900 coupled to a vertical Axio Imager 2 microscope (Zeiss). Sequential optical sections (1 μm) were acquired in Z-stacks. We used a minimum of four brain slices from each mouse. Images from damaged regions (infarct and peri-infarct) were captured at 20X magnification. The number of positive cells was expressed as the mean of the total cell number counted per mm<sup>2</sup> and it was calculated using the cell counter plugin with Fiji software. In brief, the image contrast was enhanced and then a threshold was established to eliminate the background.

**Analysis of microglial morphology**

Microglial morphology was studied on Iba-1-stained immunofluorescence images from different non-consecutive sections from Bregma +1.2 to 0.5 mm taken at 20X magnification [11]. We used cell area and number of branch points as parameters for this analysis [23]. All cells present in the study field were analysed, using a minimum of 4 non-consecutive slices per mouse. In brief, the image contrast was enhanced and then a threshold was established to eliminate the background.

**Statistical analysis**

All statistical analyses were performed with GraphPad Prism 8.0 (GraphPad Prism Software®). Data are represented as mean ± SEM (standard error of the mean). First, normal distribution of data was checked using

the Shapiro–Wilk test. Two-way analysis of variance (ANOVA), followed by post hoc multiple comparisons using Bonferroni correction, was performed to compare more than two experimental groups. The unpaired t-test was used to compare two groups. All statistical tests were performed in a two-tailed manner. Data were considered statistically significant at  $p \leq 0.05 = *$ ,  $p \leq 0.01 = **$ ,  $p \leq 0.001 = ***$ .

**Results**

**Rapamycin reduces the volume of ischemic lesions**

The MRI analysis after MCAO induction showed that rapamycin administration significantly reduced lesion volume. MCAO induced a lesion of  $17.4 \pm 1.7 \text{ mm}^3$  and rapamycin-treated ischemic mice showed a decrease in lesion volume compared to untreated counterparts (MCAO + R<sub>pre</sub>  $11.4 \pm 1.6 \text{ mm}^3$ ,  $p \leq 0.05$ ; MCAO + R<sub>post</sub>  $9.6 \pm 1.5 \text{ mm}^3$ ,  $p \leq 0.01$  vs. MCAO). No differences were observed regarding the timing of rapamycin administration (Fig. 1A, B).

**Rapamycin decreases mTORC1 activity in microglia after MCAO**

Next, we analysed mTORC activity in brain tissue. We quantified the total amount and the phosphorylated levels of the main players of the mTORC1 pathway (see Fig. 2A) to infer the activity levels of mTORC1 and mTORC2. To this end, we assessed the levels of Akt p-Ser473, which indicates mTORC2 activity, the levels

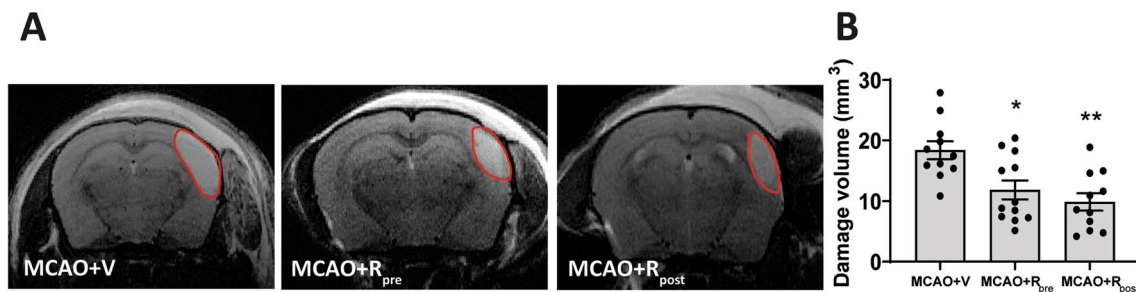


**Fig. 1** Rapamycin reduces volume of ischemic lesion. **A** Representative MRI images showing the lesion volume after 24 h of MCAO induction. The red line delineates the lesioned area. **B** Graphical quantification of lesion volumes. Data represent means ± SEM (Ordinary one-way ANOVA \*  $p \leq 0.05$ , \*\*  $p \leq 0.01$ ). MCAO + V n = 11; MCAO + R<sub>pre</sub> n = 12; MCAO + R<sub>post</sub> n = 11 (V = vehicle; R = rapamycin)

(See figure on next page.)

**Fig. 2** Rapamycin decreases mTORC1 activity in tissue after MCAO **A** Schematic representation of the mTORC1 pathway. **B** Representative Western Blot images of the analysed extracts proteins from mice cerebral cortex. Immunodetections were performed using antibodies against total Akt, Akt p-Ser473, total mTOR, mTOR p-Ser2448, total P70S6K, P70S6K p-Thr389 and B-Actin, as a loading control. **C–H** Graphical quantification of immunodetection by Western Blot. Data are normalized against B-Actin and expressed as the percentage of variation versus sham. Graph values represent means ± SEM (Ordinary one-way ANOVA \*  $p \leq 0.05$ ; \*\*  $p \leq 0.01$ ; \*\*\*  $p \leq 0.001$ . Unpaired t-test +  $p \leq 0.05$ ; ++  $p \leq 0.01$ ; +++  $p \leq 0.001$ ). Sham + V n = 4–5, Sham + R n = 4–5, MCAO + V n = 5; MCAO + R<sub>pre</sub> n = 4–5 and MCAO + R<sub>post</sub> n = 4–5 (V = vehicle; R = rapamycin). \* vs Sham and + vs MCAO + V group



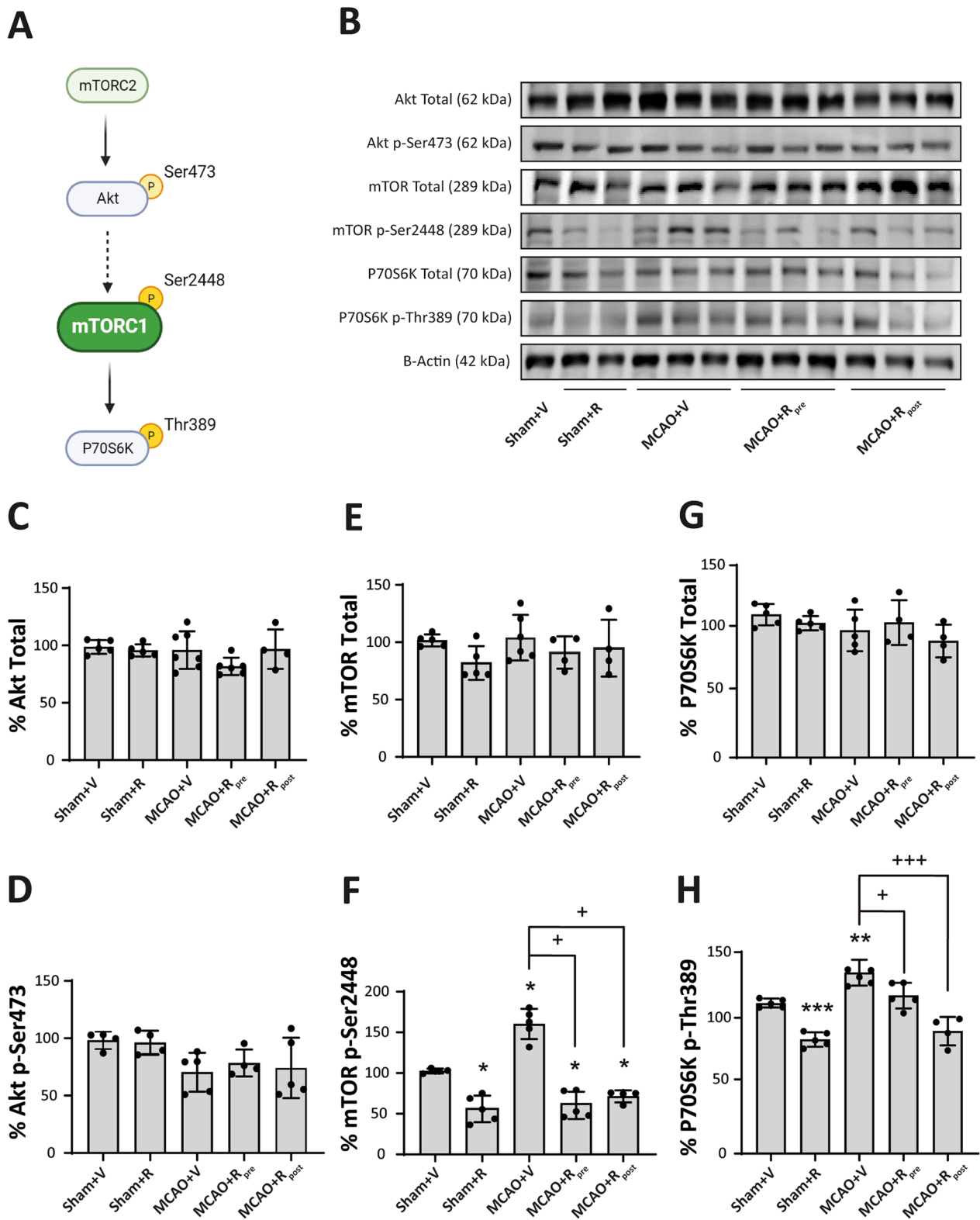


**Fig. 2** (See legend on previous page.)

of mTOR p-Ser2448 itself and P70S6K p-Thr389, the principal target of mTORC1 [43].

No variations in the levels of total Akt (Fig. 2B, C), Akt p-Ser473 (Fig. 2B–D), total mTOR (Fig. 2B–E), or total P70S6K p-Thr389 (Fig. 2B–G) were observed in any of the experimental groups. Rapamycin-treated sham mice showed a significant reduction in phosphorylation levels of mTOR p-Ser2448 ( $55.9 \pm 7.23\%$ ,  $p \leq 0.001$ ) (Fig. 2B–F) and P70S6K p-Thr389 ( $68.2 \pm 3.0\%$ ,  $p \leq 0.05$ ) (Fig. 2B–H) compared to untreated counterparts. These data confirm that rapamycin administration downregulates mTORC1 but not mTORC2 activity in the brain.

The MCAO group showed an increase in the levels of both phospho-epitopes compared to sham mice (p-mTOR:  $55.9 \pm 7.3\%$ ,  $p \leq 0.05$ ; p-P70S6K:  $68.2 \pm 3\%$ ,  $p \leq 0.01$ ) (Fig. 2B–F and B–H). Rapamycin administration pre- and post-MCAO triggered a significant reduction in p-mTOR (MCAO + R<sub>pre</sub>:  $103.3 \pm 7.2\%$ ,  $p \leq 0.05$ ; MCAO + R<sub>post</sub>:  $71.4 \pm 3.7\%$ ,  $p \leq 0.01$ ) and p-P70S6K (MCAO + R<sub>pre</sub>:  $109.4 \pm 5.4\%$ ,  $p \leq 0.05$ ; MCAO + R<sub>post</sub>:  $76 \pm 6.7\%$ ,  $p \leq 0.01$ ) levels compared to the untreated ischemic group (Fig. 2B–F and 2B–H). No differences were observed in mTOR phosphorylation levels regarding the timing of drug administration (Fig. 2B–F). However, P70S6K p-Thr389 levels showed a large decrease when rapamycin was administered post-surgery compared to pre-surgery ( $76 \pm 6.7\%$ ,  $p \leq 0.01$ ) (Fig. 2B–H).

Next, we sought to elucidate the microglial contribution to increased mTORC1-activity after stroke in brain lysates. To this end, we examined the phosphorylation levels of S6 ribosomal protein, a direct target of mTORC1/P70S6K [35], to infer mTORC1 activity in these cells by double immunofluorescence using p-S6 and Iba-1 antibodies (Fig. 3A). p-S6<sup>+</sup>/Iba-1<sup>+</sup> cells were absent in sham mice but present in the MCAO groups. The mice treated with rapamycin, pre- and post-MCAO, showed a decrease in the number of p-S6<sup>+</sup>/Iba-1<sup>+</sup> cells compared to untreated ischemic mice. No differences were observed between pre- and post-rapamycin administration (Fig. 3A). WB analyses indicated an increment in p-S6 levels after MCAO compared to sham mice ( $182.7 \pm 13.9\%$ ,  $p \leq 0.001$ ) (Fig. 3B–C). Rapamycin reduced p-S6 levels in treated sham mice compared to untreated ones ( $39.9 \pm 2.9\%$ ,  $p \leq 0.001$ ) (Fig. 3B–C). Similarly, both rapamycin-treated ischemic mouse groups showed a significant reduction in p-S6 levels compared to untreated ischemic (MCAO + R<sub>pre</sub>:  $62.2 \pm 2.8$ ,  $p \leq 0.001$ ; MCAO + R<sub>post</sub>:  $43.1 \pm 4.4\%$ ,  $p \leq 0.001$ ), without no differences between the drug administration times (Fig. 3B–C). These data suggest that the mTORC1 activation observed by WB could be related to an increase in the activity of the PI3K/Akt/mTORC1 pathway in microglia.

### Rapamycin reduces neuronal loss after MCAO

We studied the impact of mTORC1 inhibition pre- and post-MCAO on neuronal survival. To this end, we performed an immunohistochemistry assay using the NeuN antibody to quantify the number of NeuN<sup>+</sup> cells in the damaged area (see Additional file 2: Fig. S1B). Rapamycin treatment did not alter the number of NeuN<sup>+</sup> cells in sham mice. MCAO reduced the total number of NeuN<sup>+</sup> cells in the whole damaged area compared to sham mice ( $490 \pm 26$  cells/mm<sup>2</sup>,  $p \leq 0.001$ ) (Fig. 4A, B). Regional analysis showed a greater decrease in the number of NeuN<sup>+</sup> cells in the infarct zone ( $193 \pm 19$  cells/mm<sup>2</sup>,  $p \leq 0.001$ ) than in the peri-infarct region ( $297 \pm 19$  cells/mm<sup>2</sup>,  $p \leq 0.001$ ) (Fig. 4A–C). MCAO mice treated with rapamycin showed a significant reduction in the loss of neurons throughout the damaged area compared to untreated ischemic, regardless of the time of drug administration (MCAO + R<sub>pre</sub>:  $672 \pm 41$  cells/mm<sup>2</sup>,  $p \leq 0.05$ ; MCAO + R<sub>post</sub>:  $639 \pm 34$  cells/mm<sup>2</sup>,  $p \leq 0.01$ ) (Fig. 4A, B). In both rapamycin-treated ischemic groups, a further reduction in the number of NeuN<sup>+</sup> cells in the infarct zone were observed (Fig. 4A, C). No differences were found between the times of drug administration (Fig. 4B, C). The data obtained from the WB analysis confirmed the histological results. MCAO significantly reduced NeuN levels compared to untreated sham mice ( $39.6 \pm 3.7\%$ ,  $p \leq 0.001$ ), and rapamycin-treated ischemic mice showed an increase in total NeuN levels compared to untreated ischemic counterparts, both pre ( $67.8 \pm 3.6\%$ ,  $p \leq 0.001$ ) and post ( $60.5 \pm 1.9\%$ ,  $p \leq 0.001$ ) ischemic injury. No differences were observed between the times of rapamycin administration (Fig. 4D, E). These results suggest that mTORC1 inhibition prevents neuronal loss after ischemia.

### mTORC1 inhibition drives changes in microglial density and morphology after MCAO

Next, we performed immunohistochemistry on brain slices using the Iba-1 antibody to address the effect of mTORC1 inhibition specifically in microglia after MCAO. We used two distinct parameters to analyse the microglial response, namely the total number of Iba-1<sup>+</sup> cells and the total stained area. In sham groups, rapamycin treatment did not affect either parameter (Fig. 5B, C). In contrast, MCAO significantly increased both ( $762 \pm 42$  cells/mm<sup>2</sup>,  $p \leq 0.01$ ) ( $400.3 \pm 9.8\%$ ,  $p \leq 0.001$ ) compared to untreated sham mice (Fig. 5B, C). Rapamycin-treated ischemic mice showed a reduction in the number of Iba-1<sup>+</sup> cells (MCAO + R<sub>pre</sub>:  $560 \pm 30$  cells/mm<sup>2</sup>,  $p \leq 0.001$ ; MCAO + R<sub>post</sub>:  $540 \pm 27$  cells/mm<sup>2</sup>,  $p \leq 0.001$ ) and the stained area (MCAO + R<sub>pre</sub>:  $256.3 \pm 9.3\%$ ,  $p \leq 0.01$ ; MCAO + R<sub>post</sub>:  $277.3 \pm 8.4\%$ ,  $p \leq 0.001$ ) compared to untreated ischemic counterparts

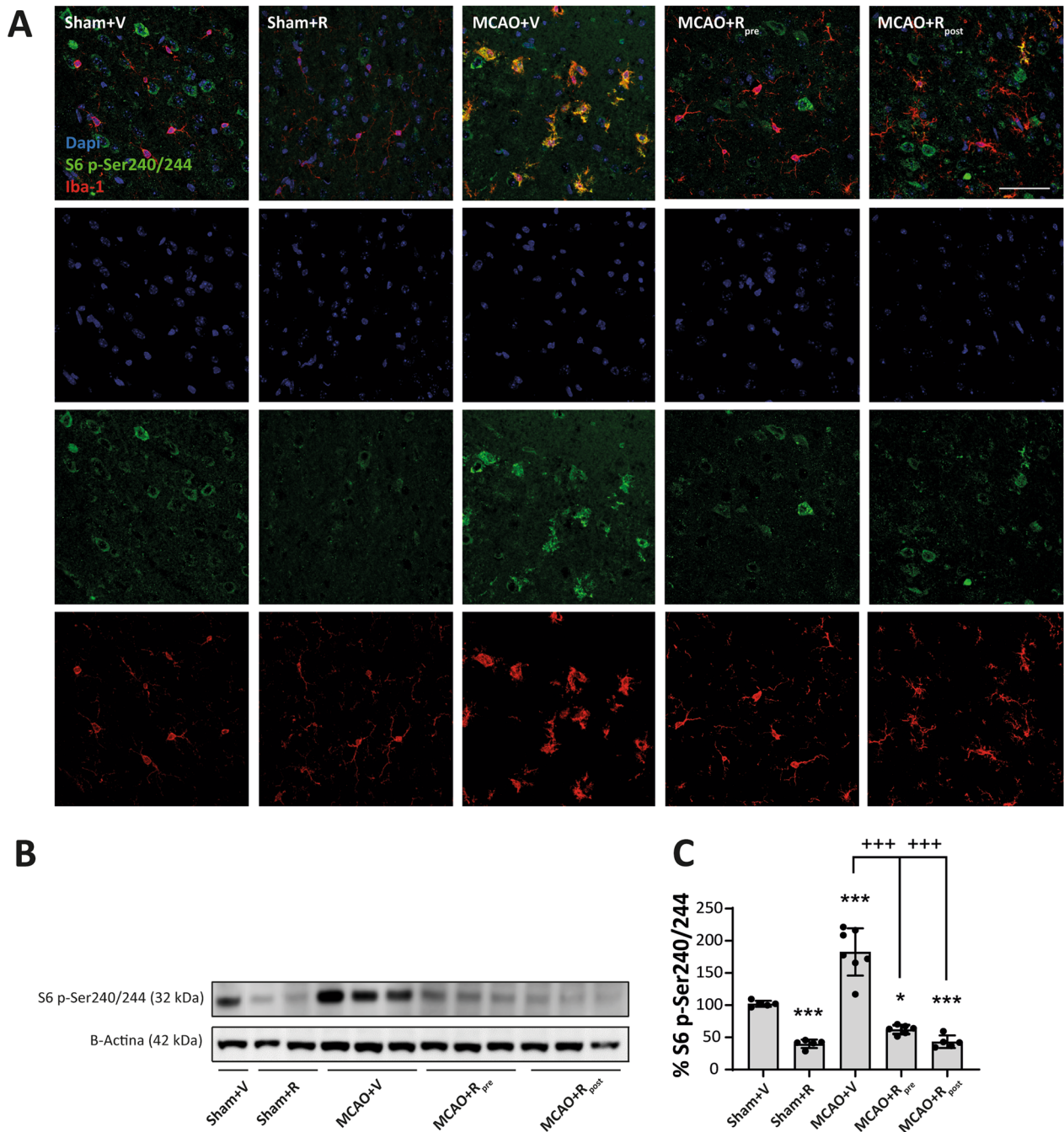


**Fig. 3** Rapamycin reduce mTORC1 activity in microglia after MCAO. **A** Representative confocal immunofluorescence images. Staining was performed using Dapi (blue), S6 p-Ser240/244 (green) and Iba-1 (red) antibodies. Scale bar: 50  $\mu$ m. **B** Representative Western Blot images of the analysed extracts proteins from mice cerebral cortex. Immunodetections were performed using antibodies against S6 p-Ser240/244 and B-Actina, as a loading control. **C** Graphical quantification of immunodetection by Western Blot. Data are normalized against B-Actina and expressed as the percentage of variation versus sham. Graph values represent means  $\pm$  SEM (Ordinary one-way ANOVA \*  $p \leq 0.05$ ; \*\*  $p \leq 0.01$ ; \*\*\*  $p \leq 0.001$ . Unpaired t-test +  $p \leq 0.05$ ; ++  $p \leq 0.01$ ; +++  $p \leq 0.001$ ). Sham +V n = 5, Sham +R n = 5, MCAO +V n = 7; MCAO +R<sub>pre</sub> n = 6 and MCAO +R<sub>post</sub> n = 5 (V = vehicle; R = rapamycin). \* vs Sham +V and + vs MCAO +V group



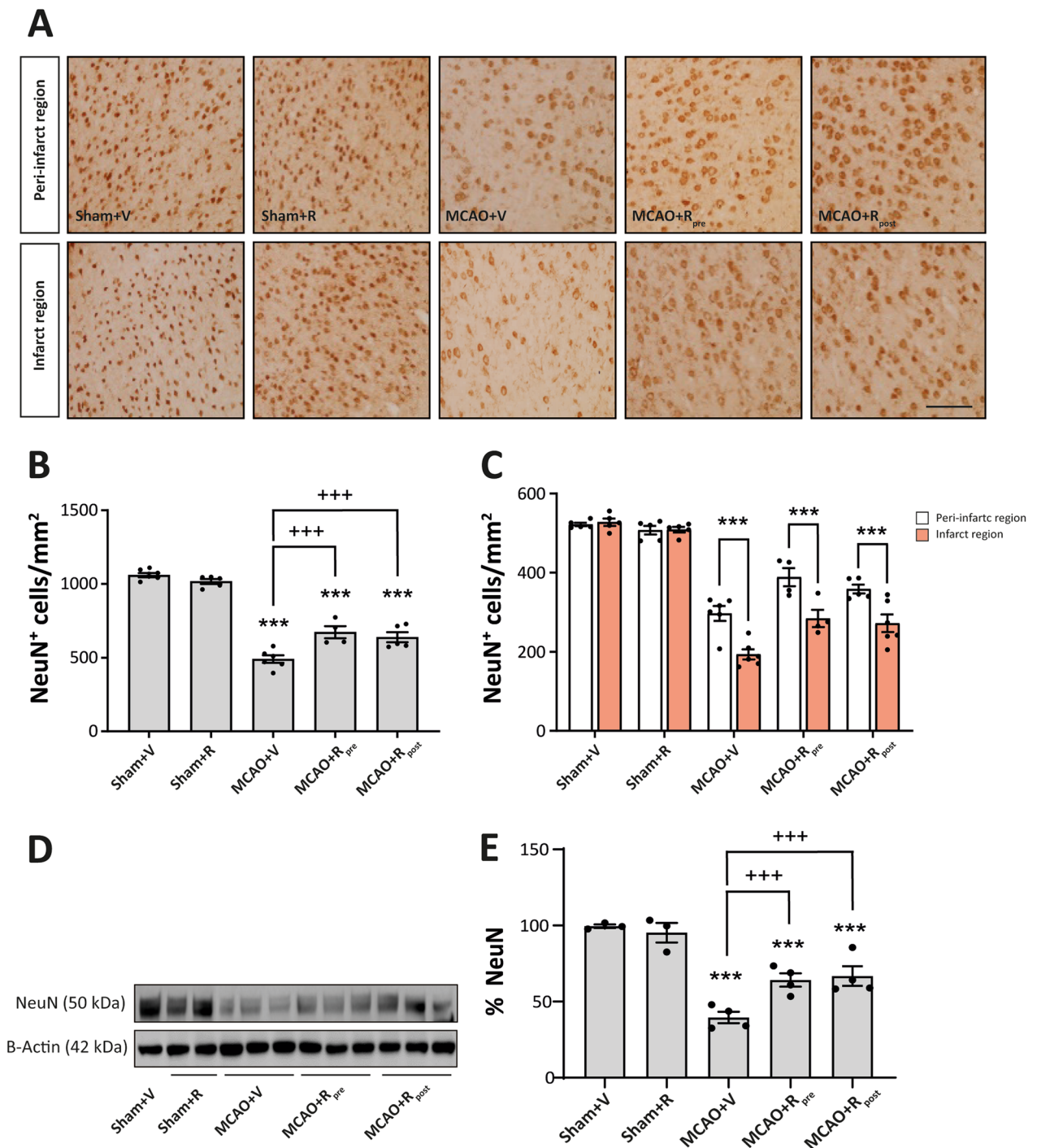


**Fig. 4** Rapamycin reduces neuronal loss after MCAO. **A** Representative immunohistochemical images from cortex infarcted area and cortex peri-infarct region (coronal section, 10  $\mu$ m). Staining was performed used NeuN antibody. Scale bar: 25  $\mu$ m. **B** Graphical quantification of NeuN<sup>+</sup> cell counting across the entire damaged cortical region. **C** Graphical quantification of NeuN<sup>+</sup> cell counting, distinguishing between the two damaged regions (white bars represent peri-infarct region whereas red bars represent infarcted area). **D** Representative Western Blot images of the analysed extracts proteins from mice cerebral cortex. Immunodetections were performed using antibodies against NeuN and B-Actin, as a loading control. **E** Graphical quantification of immunodetection by Western Blot. Data are normalized against B-Actin and expressed as the percentage of variation versus sham. Graph values represent means  $\pm$  SEM (Ordinary one/two-way ANOVA \*  $p \leq 0.05$ ; \*\*  $p \leq 0.01$ ; \*\*\*  $p \leq 0.001$ . Unpaired t-test +  $p \leq 0.05$ ; ++  $p \leq 0.01$ ; +++  $p \leq 0.001$ ). Sham + V n = 5, Sham + R n = 5, MCAO + V n = 7; MCAO + R<sub>pre</sub> n = 6 and MCAO + R<sub>post</sub> n = 5 (V = vehicle; R = rapamycin). \* vs Sham + V and + vs MCAO + V group



and no differences were observed between the times of rapamycin administration (Fig. 5B, C). No significant differences were observed between the damaged area of the infarct zone and peri-infarct region in any of the parameters analysed (data not shown).

Microglial activation is a highly dynamic process that involves changes in cellular morphology. These variations have been associated with the extent and duration of ischemic damage [17]. Thus, we examined the effect of mTORC1 inhibition on the number of branch points and cell area of microglia [23], addressing the infarct zone and peri-infarct region separately. Rapamycin administration in sham mice did not cause any variations in the number of branch points or cell area in either of the damaged regions (Fig. 5E, F). In contrast, mice subjected to MCAO showed an increase in both parameters compared to sham mice. In the peri-infarct region, Iba-1<sup>+</sup> cell showed a ramified morphology with an increase in the number of branch points ( $6.9 \pm 0.1$ ,  $p \leq 0.001$ ) and cellular area ( $1.03 \times 10^6 \pm 2.8 \times 10^4 \mu\text{m}^2$ ,  $p \leq 0.001$ ) compared to the infarct zone (Fig. 5E, F). In the latter, Iba-1<sup>+</sup> cells showed an amoeboid morphology with a significant reduction in both parameters (Branch points:  $4.2 \pm 0.25$ ,  $p \leq 0.001$ . Cell area:  $5.8 \times 10^5 \pm 2.6 \times 10^4 \mu\text{m}^2$ ,  $p \leq 0.001$ ) (Fig. 5E, F).

Rapamycin-treated ischemic mice showed a significant decrease in both parameters compared to untreated ischemic counterparts. No differences were observed between the two damaged regions or between the times of rapamycin administration (Fig. 5E, F). Slightly branched morphologies were observed compared to highly ramified morphologies MCAO in the peri-infarct region.

Astrocytes are another cell type involved in the inflammatory response. Analysis of the astrocytic response revealed that MCAO significantly increased the levels of GFAP ( $165.1 \pm 11.4\%$ ,  $p \leq 0.001$ ) compared to the sham condition. The levels of GFAP in rapamycin-treated ischemic mice (pre- or post-MCAO) did not differ from those of untreated ischemic (Additional file 2: Fig. S2A–C).

### mTORC1 inhibition ameliorates microglia reactivity after MCAO

To determine microglia reactivity after MCAO, we analysed soluble-TREM2 (sTREM2) and iNOS. The results refer to the entire region of damaged cerebral cortex because we did not find differences between the infarct zone and the peri-infarct region (data not shown). sTREM2 has been related to microglia activation in various neuroinflammation backgrounds [36]. WB analysis showed an increase in sTREM2 levels after MCAO compared to untreated sham mice ( $140.2 \pm 8.4\%$ ,  $p \leq 0.001$ ) (Fig. 6A, B). Rapamycin-treated ischemic mice showed a significant reduction in sTREM2 levels compared to untreated ischemic (MCAO + R<sub>pre</sub>:  $112.7 \pm 4.6\%$ ,  $p \leq 0.001$ ; MCAO + R<sub>post</sub>:  $87.20 \pm 8.3\%$ ,  $p \leq 0.05$ ) (Fig. 6A, B). This decrease was more marked when rapamycin was injected after MCAO induction. Rapamycin administration had no effect on the sham group (Fig. 6A, B). In addition, we performed double immunofluorescence staining using Iba-1 and sTREM2 antibodies. We observed that MCAO increased the number of sTREM2<sup>+</sup>/Iba-1<sup>+</sup> cells compared to the control (Fig. 6C). The two ischemic groups treated with rapamycin showed a reduction in the number of sTREM2<sup>+</sup>/Iba-1<sup>+</sup> cells compared to untreated counterparts (Fig. 6C). In sham mice, rapamycin administration did not alter the number of sTREM2<sup>+</sup>/Iba-1<sup>+</sup> cells (Fig. 6C).

To identify the effect of rapamycin on the abundance of microglia with the pro-inflammatory phenotype, we performed double immunofluorescence staining using antibodies against iNOS and Iba-1. Rapamycin administration did not alter the number of double-positive cells in sham mice. However, ischemic mice showed an increase in the number of iNOS<sup>+</sup>/Iba-1<sup>+</sup> cells compared to untreated sham mice (Fig. 7A). Rapamycin administration both pre and post-MCAO restored this parameter to sham values (Fig. 7A). No differences were observed between rapamycin administration pre and post-MCAO (Fig. 7A).

These results strongly support the notion that mTORC1 inhibition by rapamycin, both pre and post-MCAO, reduces pro-inflammatory microglia reactivity.

(See figure on next page.)

**Fig. 5** mTORC1 inhibition in microglia drives changes in their density and morphology after MCAO. **A** Representative immunohistochemical images from the entire damage area (coronal section, 10  $\mu\text{m}$ ). Staining was performed using Iba-1 antibody. Scale bar: 25  $\mu\text{m}$ . **B** Graphical representation of Iba-1<sup>+</sup> cell counting and **C** graphical representation of Iba-1<sup>+</sup> stained damage area. **D** Representative confocal immunofluorescence images from peri-infarct and infarct area. Staining was performed using Dapi (blue) and Iba-1 (red) antibody. Scale bar: 5  $\mu\text{m}$ . **E** Graphical representation of the quantification of branching points and the **F** area occupied by each Iba-1<sup>+</sup> cell in both damaged regions (white bars represent peri-infarct region whereas red bars represent infarcted area). Ordinary one/two-way ANOVA \*  $p \leq 0.05$ ; \*\*  $p \leq 0.01$ ; \*\*\*  $p \leq 0.001$ . Unpaired t-test +  $p \leq 0.05$ ; ++  $p \leq 0.01$ ; +++  $p \leq 0.001$ . Sham + V n = 5, Sham + R n = 5, MCAO + V n = 7; MCAO + R<sub>pre</sub> n = 6 and MCAO + R<sub>post</sub> n = 5 (V = vehicle; R = rapamycin). + vs Sham + V (peri-infarct region), # vs Sham + V (infarct region) and \* vs same experimental group

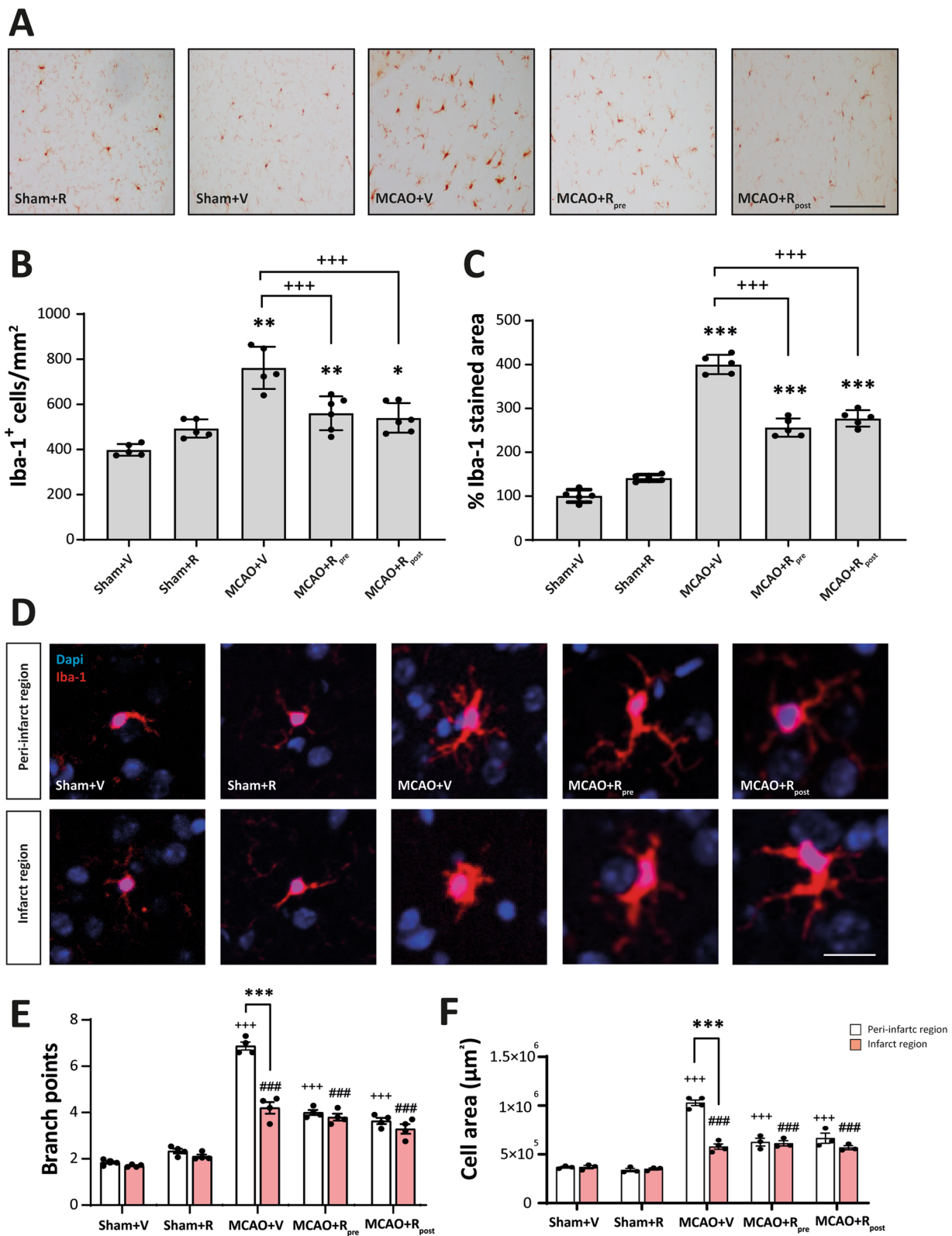


**Fig. 5** (See legend on previous page.)

## Discussion

After ischemic damage, the brain tissue generates a stereotypic replay trying to establish the normal physiology, if possible. When the recovery is not possible or correct the ischemic process may turn into a complex and multifactorial neurodegenerative disease associated with a large inflammatory process [44, 52]. Several authors support the notion that neuroinflammation plays a key role in the recovery of CNS homeostasis by modulating some brain repair mechanisms [34]. However, a sustained response over time may contribute to the development of psychiatric disorders and neurodegenerative diseases [48, 54]. The therapeutic approaches used to reduce ischemic damage involve recanalization strategies, including the administration of antithrombotic agents and surgical removal of the thrombus to rescue less damage neurons in the peri-infarct area. The restoration of blood flow can mitigate the effects of ischemia only when performed a few hours after onset of the first symptoms. However, despite the beneficial effects of this approach, it is not suitable for all patients and does not reduce subsequent neurodegeneration [49, 51]. In this context, considerable research efforts focus on the search for pharmacological alternatives to improve ischemic damage in these patients and enhance the effects of reperfusion.

Here we used a murine model of transient focal cerebral ischemia by intra-vascular thrombin injection, which has proven to be a suitable model to analyse the acute phase of ischemia in which neuroinflammation has been reported [38]. As a therapeutic approach, we tested rapamycin, a known inhibitor of mTORC1, administered pre- and post-MCAO.

A pivotal player in the PI3K/Akt/mTORC1 survival pathway, the mTOR protein is associated with neuroprotection in the context of cerebral ischemia through its role in the maintenance of neuronal homeostasis [8, 9]. However, there is less information about its possible role in glial cells such as astrocytes and microglia. Recent studies suggest that the PI3K/Akt/mTORC1 pathway is involved in microglia activation and that the dysregulation of this pathway contributes to alterations of the neuroinflammatory response [5].

Our MRI data indicated that MCAO resulted in a considerable volume of lesion (18 mm<sup>3</sup>) in the parietal cortex, accompanied by a marked decrease in the number of neurons. The latter decrease was more pronounced in the infarct zone than in the peri-infarct region, as reported by others [7]. Cerebral ischemia triggers an early gliosis, including microglia and astrocytes as occurs in many brain insults. Although the astrocyte response is later than the microglial response, in our model we detected an increase in GFAP levels distributed around the damaged area, thereby providing evidence of a response by these cells. Consistent with previous reports describing the microglial response as one of the earliest events after cerebral ischemia, we observed an increase in both the number of Iba-1<sup>+</sup> cells and their stained area, thereby confirming the presence of reactive microglial throughout the entire damaged area [46]. In parallel, the biochemical analysis revealed an increase in the phosphorylation of mTOR and P70S6K, without any variations in their total amounts. Moreover, this analysis did not detect changes in either the phosphorylation or total levels of Akt. These data allow us to confirm that MCAO drives an increase in mTORC1 activity without affecting the basal activity of mTORC2, as reported elsewhere [4, 55]. However, other studies have described opposite results with respect to mTORC1 activity after ischemia [4, 15, 32]. The use of distinct models that included or excluded reperfusion, the duration of ischemic damage, and the time of analysis could explain the differences between the findings. In this context, to better understand the tissular response to ischemic damage and optimize strategies based on mTORC as therapeutic targets, it is important to take into account the model of ischemia used [49].

The reactive microglia has been associated with changes in the morphology and functions of this cell type. These transformations require a balance between catabolic and anabolic cellular processes, which are regulated, in part, by mTORC1 [5]. Thus, using an immunofluorescence approach, we revealed an increase in the number of p-S6<sup>+</sup>/Iba-1<sup>+</sup> cells in the whole damaged area of MCAO mice. This observation strongly supports the notion that the increase in mTORC1

(See figure on next page.)

**Fig. 6** mTORC1 inhibition reduces Iba-1<sup>+</sup>/sTREM2<sup>+</sup> after MCAO. **A** Representative Western Blot images of the analysed extracts proteins from mice cerebral cortex. Immunodetections were performed using antibodies against sTREM2 and B-Actin, as a loading control. **B** Graphical quantification of immunodetection by Western Blot. Data are normalized against B-Actin and expressed as the percentage of variation versus sham. Graph values represent means ± SEM (Ordinary one-way ANOVA \*  $p \leq 0.05$ ; \*\*  $p \leq 0.01$ ; \*\*\*  $p \leq 0.001$ . Unpaired t-test +  $p \leq 0.05$ ; ++  $p \leq 0.01$ ; +++  $p \leq 0.001$ ). Sham + V  $n = 5$ , Sham + R  $n = 5$ , MCAO + V  $n = 5$ ; MCAO + Rpre  $n = 5$  and MCAO + Rpost  $n = 5$  (V = vehicle; R = rapamycin). \* vs Sham + V and + vs MCAO + V group. **C** Representative confocal immunofluorescence images from the entire damage area. Staining was performed using Dapi (blue), sTREM2 (green) and Iba-1 (magenta) antibodies. Scale bar: 25  $\mu\text{m}$



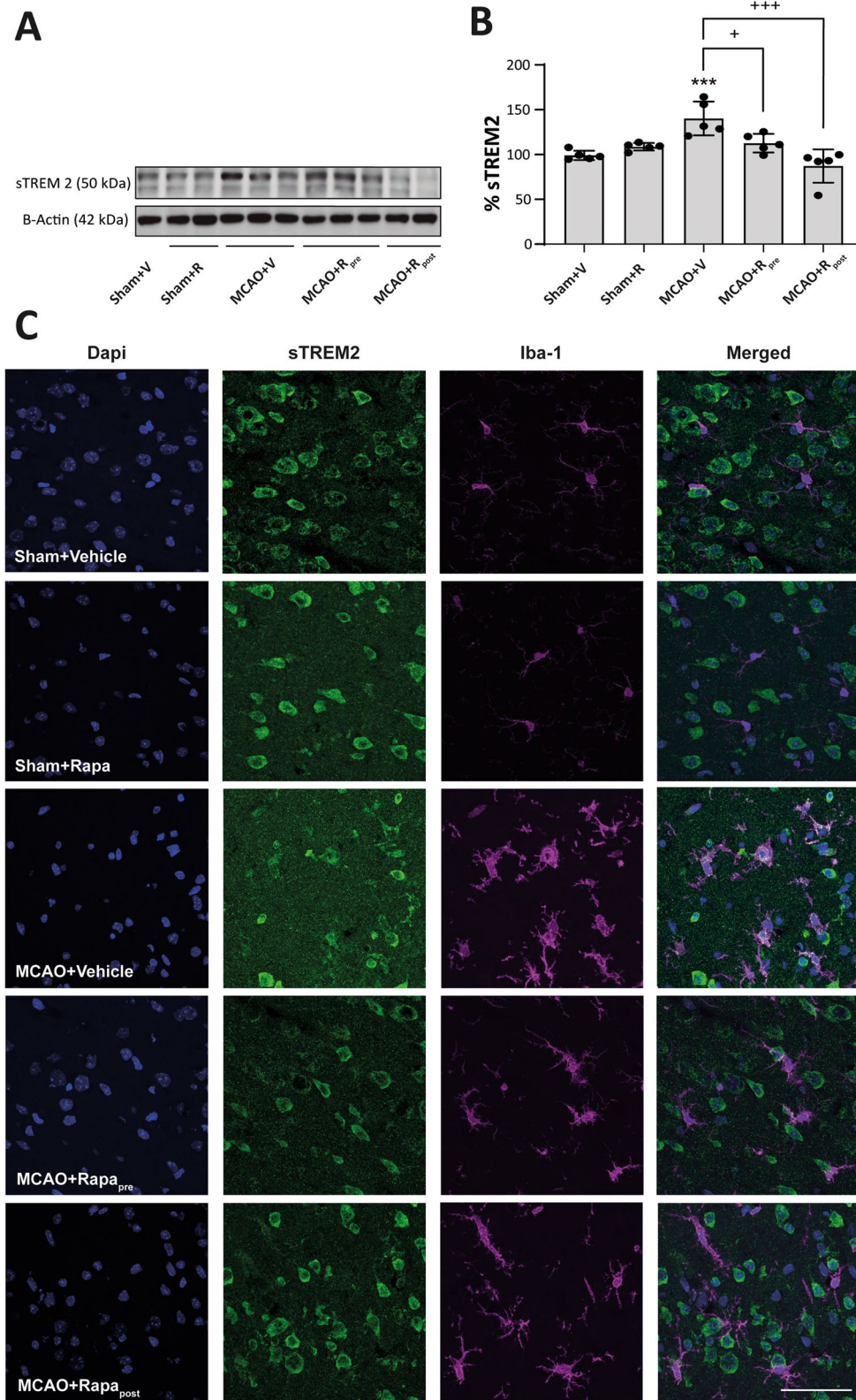


**Fig. 6** (See legend on previous page.)



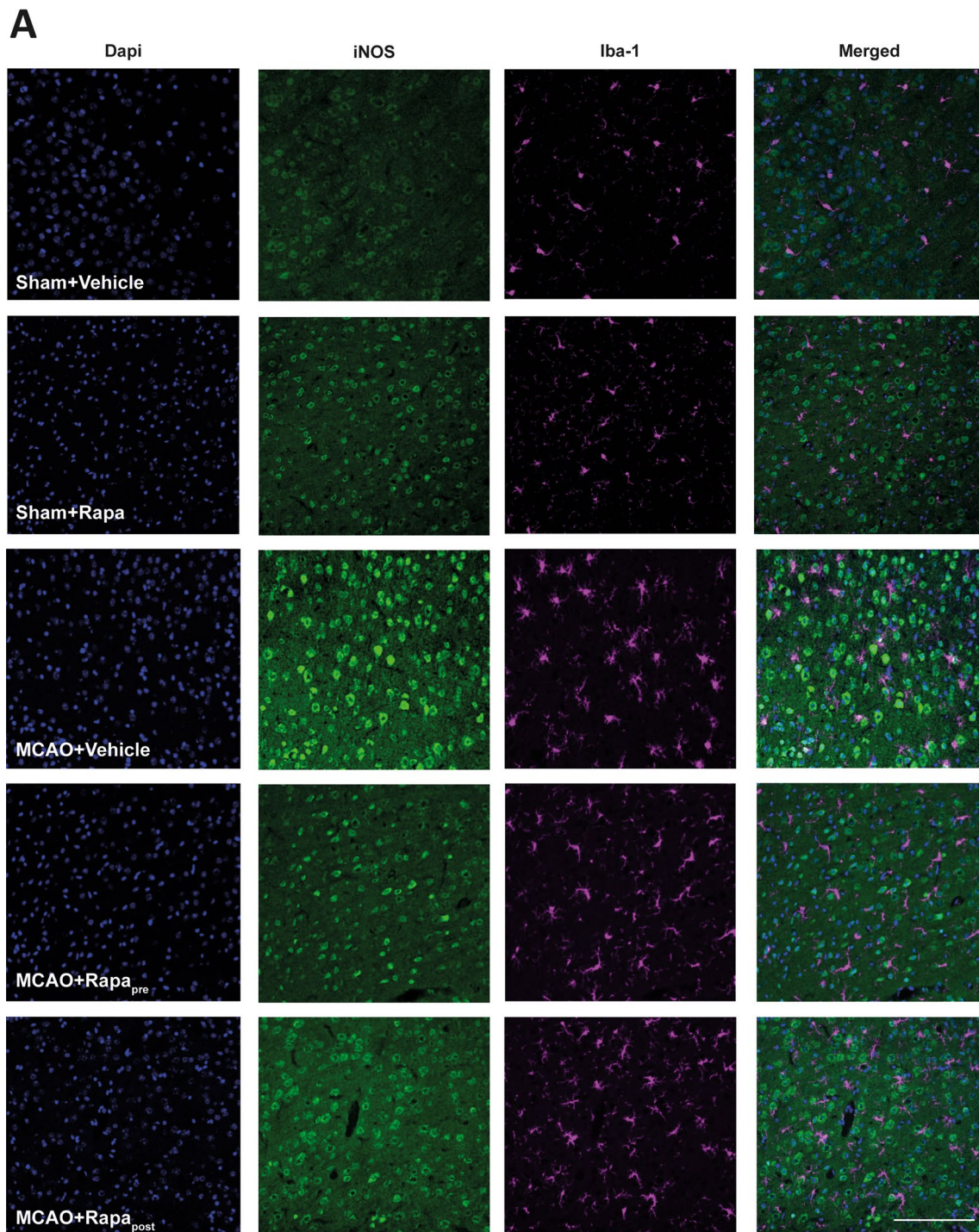


**Fig. 7** mTORC1 inhibition reduces Iba-1<sup>+</sup>/iNOS<sup>+</sup> after MCAO. **A** Representative confocal immunofluorescence images from the entire damage area. Staining was performed using Dapi (blue), iNOS (green) and Iba-1 (magenta) antibodies. Scale bar: 50 μm

activity, observed by WB, is due mainly to microglia. In addition, the morphological heterogeneity of the microglial response has been associated with the extent and duration of ischemic damage, and with the

characteristics of the brain region monitored by these cells [31, 37]. Our data showed that the predominant microglial phenotype after MCAO differed between the infarct zone and peri-infarct region, with amoeboid

microglia being most abundant in the former and highly branched microglia in the latter, as reported previously [45]. Furthermore, microglia activation involves polarization to the M1 pro-inflammatory or M2 anti-inflammatory phenotype. Despite this binary classification, there is evidence that supports the coexistence of a heterogeneous reactive microglia population [13, 19]. In the present study, we analysed microglia reactivity using sTREM2 and iNOS. The former is a transmembrane receptor expressed mainly by immune cells and by reactive microglia in the CNS [36]. Some authors have reported an association between sTREM2 levels and the prognosis of ischemia [22, 29]. On the other hand, iNOS produces nitric oxide, which promotes neuronal death after stroke [50]. Our data showed that MCAO triggers an increase in both markers in microglia, accompanied by an increase in the number of p-S6<sup>+</sup>/Iba-1<sup>+</sup> in the damaged area. Based on our findings, we propose that, post-MCAO, mTORC1 activity mediates the early state of reactive microglia that could contribute to the detrimental effects of inflammation. Thus, we studied whether mTORC1 inhibition confers neuroprotection in our ischemia model. Rapamycin has been used in clinical practice for several decades due to its immunosuppressive properties, and it shows promising results in some ischemic pathologies [16, 33]. However, there are controversial results about dosage and timing of administration. Several studies derived from meta-analysis have shown that low doses of rapamycin have greater efficacy against ischemic damage compared to high ones, showing a reduction in the volume of damage and neurological improvement in animals [1]. Whereas mTORC1 is highly sensitive to rapamycin, mTORC2 inhibition requires higher doses or prolonged exposure to this drug [10, 47]. Therefore, high rapamycin dosages exacerbate autophagy induction and mTORC2 inhibition. The regulation of neuronal survival pathways is under mTORC2 governance. Therefore, the maintenance of basal levels of this complex and/or its increase after cerebral ischemia could be a fundamental approach for neuronal survival and the reduction of the volume of damage [1, 21]. In this context, the inhibition of both mTORC1 and mTORC2 by rapalink-1 increases the volume of the ischemic lesion [3, 4]. In contrast, our results showed that 20 mg/kg rapamycin administered pre- or post-MCAO decreased the volume of damage by 35–45%. Our WB data showed that rapamycin did not modify Akt p-Ser473 levels in the sham group, thereby suggesting that this dosage of rapamycin is not sufficient to inhibit mTORC2 activity. In contrast, we observed that rapamycin caused a significant reduction in p-mTOR and p-P70S6K levels

after MCAO—findings consistent with those reported in other studies [27, 55].

Regarding the time of rapamycin administration, the present study and another carried out by Wu and colleagues [53] are the only ones to compare rapamycin administration pre- and post-ischemic damage. Our data showed that, for both rapamycin administration approaches, damage volume and neuronal loss were markedly lower compared to the vehicle-treated ischemic group, with no difference between the administration times used [53]. However, at the biochemical level, rapamycin administration post-damage further reduced mTORC1 activity than at 48 h before ischemia, as reflected by lower levels of P70S6K phosphorylation by mTORC1 in the MCAO + R<sub>post</sub> group. The differences observed could be attributed to the effective concentration of rapamycin in the brain, a parameter related to the time between drug administration and euthanasia of the animals.

mTORC1 inhibition led to a decrease in both the number of Iba-1<sup>+</sup> cells and the intensity of Iba-1 staining in the damaged area, a finding consistent with other studies [25]. The analysis of microglia morphology showed that mTORC1 inhibition reduced the branching and area of Iba-1<sup>+</sup> cells. Accordingly, after rapamycin treatment, we observed slightly branched morphologies in the damaged area compared to highly branched microglia in the perinfarct region and amoeboid morphologies in the infarct zone described in untreated ischemic mice. The present study is the first to analyse the effects of rapamycin-induced mTORC1 inhibition on changes in microglial morphology. In addition, these morphological changes were associated with a significant reduction in sTREM2 and iNOS levels in microglia.

## Conclusions

On the basis of our results, we conclude that mTORC1 inhibition reduces the reactivity and the pro-inflammatory phenotype of microglia, thereby decreasing neuronal death and ischemic lesion volume. Several working hypotheses can be put forward to explain these findings. For instance, it is tempting to propose that the mTORC1-P70S6K-S6 pathway regulates microglia activation after the induction of cerebral ischemia and that the modulation of this activation by rapamycin reduces microglial reactivity and neuronal death. However, we cannot discard a complementary effect of rapamycin on neurons and/or other cells in the damaged area.

Finally, taken together, our data demonstrate that the use of specific mTORC1 inhibitors during the acute phase of cerebral ischemia has a neuroprotective effect, reducing the inflammatory microglial response. Given that rapamycin administration pre- and post-MCAO

induction had similar effects with respect to neuronal protection, the administration of rapamycin or new rapalog emerges as a potential therapeutic approach to tackle the acute phase of cerebral ischemia. Such a therapeutic strategy could be easily tested on patients as rapamycin is already authorised for the treatment of other human pathologies.

#### Abbreviations

Akt	Protein kinase B
CNS	Central Nervous System
iNOS	Inducible Nitric Oxide Synthase
MCAO	Middle Cerebral Artery Occlusion
MRI	Magnetic Resonance Imaging
mTOR	Mammalian target of rapamycin
mTORC1	Mammalian target of rapamycin complex 1
mTORC2	Mammalian target of rapamycin complex 2
P70S6K	Ribosomal protein S6 kinase
R	Rapamycin
S6	Ribosomal protein S6
sTREM2	Soluble Triggering receptor expressed on myeloid cells 2 (TREM)
V	Vehicle
WB	Western Blot

#### Supplementary Information

The online version contains supplementary material available at <https://doi.org/10.1186/s13062-024-00470-5>.

**Additional file 1. Fig. S1.** Experimental design and determination of damage regions. A) Mice were randomly distributed into five experimental groups. Sham groups were injected with the vehicle solution or rapamycin 48 hours before MCAO simulation. MCAO+V group was injected with the vehicle solution 48 hours before the surgery. MCAO+Rpre group was injected with rapamycin 48 hours before the surgical procedure, while the MCAO+Rpost group was injected with rapamycin 20 minutes after the surgery. Twenty-four hours following the MCAO simulation or induction, brain damage was assessed by MRI. Then animals were euthanized collecting brains to perform the corresponding analysis. B) According to the MRI images, infarcted area affects to M1/M2 cortex (Field 2) whereas the peri-infarct area corresponds to the S1 cortex (Field 1).

**Additional file 2. Fig. S2.** MCAO triggers astrocytic response. A) Representative immunohistochemical images from the entire damage area (coronal section 10  $\mu$ m). Staining was performed using GFAP antibody. Scale bar: 25  $\mu$ m. B) Representative Western Blot images of the analysed extracts proteins from mice cerebral cortex. Immunodetections were performed using antibodies against GFAP and B-Actin, as a loading control. C) Graphical quantification of immunodetection by Western Blot. Data are normalized against B-Actin and expressed as the percentage of variation versus sham. Graph values represent means  $\pm$  SEM (Ordinary one-way ANOVA \* $p \leq 0.05$ ; \*\* $p \leq 0.01$ ; \*\*\* $p \leq 0.001$ ). Sham+V n=5, Sham+R n=4, MCAO+V n=5; MCAO+Rpre n=5 and MCAO+Rpost n=5 (V=vehicle; R=rapamycin). \* vs Sham+V.

#### Acknowledgements

We would like to thank the Confocal Microscopy facility of the CBMSO for their assistance and support along this project. We are also thankful to the current and former members of our labs.

#### Author contributions

MVG: data acquisition, data analysis, interpretation of data and drafted the manuscript. MR: data acquisition and discussion of results and revised manuscript. GML: data acquisition, data analysis. PRM: data acquisition and data analysis. LVS: data acquisition, data analysis. DV: conception and designing of the work and revised manuscript. FW: conception and designing of the work, interpretation of data, discussion of results and substantively revised

manuscript. MJ: conception and designing of the work, interpretation of data, discussion of results and substantively revised manuscript.

#### Funding

This work was supported by grants from the Spanish FEDER/Science and Innovation Ministry I + D + i-RETOS-PID2021-124801NB-I00, I + D + i-RETOS-PID2021-124801NB-I00, I + D + i-RETOS PID2020-115876GB-I00 and Centro de Investigación Biomédica en Red sobre Enfermedades Neurodegenerativas (CIBERNED; an initiative of the ISCIII) [PI2016/01]. Institutional grants from the Fundación Ramón Areces and Banco Santander to the CBMSO are also acknowledged by FW (CBMSO). M.V.G was supported by a EMBO short-term fellowship (8665). G.M.L was supported by a Tatiana Pérez de Guzmán el Bueno fellowship 2021.

#### Availability of data and materials

The datasets used and/or analyses during the current study are available from the corresponding author on reasonable request.

#### Declarations

##### Ethics approval and consent to participate

All the animals were housed in the Animal Facility of U1237 (GIP Cycleron) with food and water ad libitum access under a 12-h light/dark cycle in a temperature-controlled environment. All care and experiments were performed following the ARRIVE guidelines (#24316) ([www.nc3rs.org.uk](http://www.nc3rs.org.uk)).

##### Consent for publication

Not applicable.

##### Competing interests

The authors declare that they have no competing interest.

Received: 2 January 2024 Accepted: 25 March 2024

Published online: 06 April 2024

#### References

- Beard DJ, Hadley G, Thurley N, Howells DW, Sutherland BA, Buchan AM. The effect of rapamycin treatment on cerebral ischemia: a systematic review and meta-analysis of animal model studies. *Int J Stroke*. 2019;14(2):137–45. <https://doi.org/10.1177/1747493018816503>.
- Chauhan A, Sharma U, Jagannathan NR, Gupta YK. Rapamycin ameliorates brain metabolites alterations after transient focal ischemia in rats. *Eur J Pharmacol*. 2015;757:28–33. <https://doi.org/10.1016/j.ejphar.2015.03.006>.
- Chi OZ, Barsoum S, Vega-Cotto NM, Jacinto E, Liu X, Mellender SJ, Weiss HR. Effects of rapamycin on cerebral oxygen supply and consumption during reperfusion after cerebral ischemia. *Neuroscience*. 2016;316:321–7. <https://doi.org/10.1016/j.neuroscience.2015.12.045>.
- Chi OZ, Liu X, Cofano S, Patel N, Jacinto E, Weiss HR. Rapalink-1 increased infarct size in early cerebral ischemia-reperfusion with increased blood-brain barrier disruption. *Front Physiol*. 2021;12: 706528. <https://doi.org/10.3389/fphys.2021.706528>.
- Chu E, Mychasiuk R, Hibbs ML, Sempke BD. Dysregulated phosphoinositide 3-kinase signaling in microglia: shaping chronic neuroinflammation. *J Neuroinflammation*. 2021;18(1):276. <https://doi.org/10.1186/s12974-021-02325-6>.
- Dirnagl U, Iadecola C, Moskowitz MA. Pathobiology of ischaemic stroke: an integrated view. *Trends Neurosci*. 1999;22(9):391–7. [https://doi.org/10.1016/s0166-2236\(99\)01401-0](https://doi.org/10.1016/s0166-2236(99)01401-0).
- Ermine CM, Bivard A, Parsons MW, Baron JC. The ischemic penumbra: from concept to reality. *Int J Stroke*. 2021;16(5):497–509. <https://doi.org/10.1177/1747493020975229>.
- Fan J, Li X, Yu X, Liu Z, Jiang Y, Fang Y, Zong M, Suo C, Man Q, Xiong L. Global burden, risk factor analysis, and prediction study of ischemic stroke, 1990–2030. *Neurology*. 2023;101(2):e137–50. <https://doi.org/10.1212/wnl.0000000000207387>.



9. Fan PL, Wang SS, Chu SF, Chen NH. Time-dependent dual effect of microglia in ischemic stroke. *Neurochem Int.* 2023;169: 105584. <https://doi.org/10.1016/j.neuint.2023.105584>.
10. Fletcher L, Evans TM, Watts LT, Jimenez DF, Digicaylioglu M. Rapamycin treatment improves neuron viability in an in vitro model of stroke. *PLoS One.* 2013;8(7): e68281. <https://doi.org/10.1371/journal.pone.0068281>.
11. Paxinos G, Franklin KB. Paxinos and Franklin's the mouse brain in stereotaxic coordinates. Cambridge: Academic press; 2019.
12. Ge P, Duan H, Tao C, Niu S, Hu Y, Duan R, Shen A, Sun Y, Sun W. TMAO promotes NLRP3 inflammasome activation of microglia aggravating neurological injury in ischemic stroke through FTO/IGF2BP2. *J Inflamm Res.* 2023;16:3699–714. <https://doi.org/10.2147/jir.S399480>.
13. Girard S, Brough D, Lopez-Castejon G, Giles J, Rothwell NJ, Allan SM. Microglia and macrophages differentially modulate cell death after brain injury caused by oxygen-glucose deprivation in organotypic brain slices. *Glia.* 2013;61(5):813–24. <https://doi.org/10.1002/glia.22478>.
14. Glass CK, Saijo K, Winner B, Marchetto MC, Gage FH. Mechanisms underlying inflammation in neurodegeneration. *Cell.* 2010;140(6):918–34. <https://doi.org/10.1016/j.cell.2010.02.016>.
15. Gu C, Yang J, Luo Y, Ran D, Tan X, Xiang P, Fei H, Lu Y, Guo W, Tu Y, Liu X, Wang H. ZNF2 attenuates focal cerebral ischemia/reperfusion injury in rats by inhibiting mTORC1-mediated autophagy. *Experiment Neurol.* 2021;342:113759. <https://doi.org/10.1016/j.expneurol.2021.113759>.
16. Hadley G, Beard DJ, Couch Y, Neuhaus AA, Adriaanse BA, DeLuca GC, Sutherland BA, Buchan AM. Rapamycin in ischemic stroke: Old drug, new tricks? *J Cereb Blood Flow Metab.* 2019;39(1):20–35. <https://doi.org/10.1177/0271678x18807309>.
17. Hernández IH, Villa-González M, Martín G, Soto M, Pérez-Álvarez MJ. Glial cells as therapeutic approaches in brain ischemia-reperfusion injury. *Cells.* 2021. <https://doi.org/10.3390/cells10071639>.
18. Jurcau A, Simion A. Neuroinflammation in cerebral ischemia and ischemia/reperfusion injuries: from pathophysiology to therapeutic strategies. *Int J Mol Sci.* 2021. <https://doi.org/10.3390/ijms23010014>.
19. Kanazawa M, Ninomiya I, Hatakeyama M, Takahashi T, Shimohata T. Microglia and monocytes/macrophages polarization reveal novel therapeutic mechanism against stroke. *Int J Mol Sci.* 2017. <https://doi.org/10.3390/ijms18102135>.
20. Karalis V, Bateup HS. Current approaches and future directions for the treatment of mTORopathies. *Dev Neurosci.* 2021;43(3–4):143–58. <https://doi.org/10.1159/000515672>.
21. Kim YS, Yoo A, Son JW, Kim HY, Lee YJ, Hwang S, Lee KY, Lee YJ, Ayata C, Kim HH, Koh SH. Early activation of phosphatidylinositol 3-kinase after ischemic stroke reduces infarct volume and improves long-term behavior. *Mol Neurobiol.* 2017;54(7):5375–84. <https://doi.org/10.1007/s12035-016-0063-4>.
22. Kwon HS, Lee EH, Park HH, Jin JH, Choi H, Lee KY, Lee YJ, Lee JH, de Oliveira FMS, Kim HY, Seo Kim Y, Kim BJ, Heo SH, Chang DI, Kamali-Moghaddam M, Koh SH. Early increment of soluble triggering receptor expressed on myeloid cells 2 in plasma might be a predictor of poor outcome after ischemic stroke. *J Clin Neurosci.* 2020;73:215–8. <https://doi.org/10.1016/j.jocn.2020.02.016>.
23. Leyh J, Paeschke S, Mages B, Michalski D, Nowicki M, Bechmann I, Winter K. Classification of microglial morphological phenotypes using machine learning. *Front Cell Neurosci.* 2021;15: 701673. <https://doi.org/10.3389/fncel.2021.701673>.
24. Li D, Wang C, Yao Y, Chen L, Liu G, Zhang R, Liu Q, Shi FD, Hao J. mTORC1 pathway disruption ameliorates brain inflammation following stroke via a shift in microglia phenotype from M1 type to M2 type. *Faseb J.* 2016;30(10):3388–99. <https://doi.org/10.1096/fj.201600495R>.
25. Li T, Pang S, Yu Y, Wu X, Guo J, Zhang S. Proliferation of parenchymal microglia is the main source of microgliosis after ischaemic stroke. *Brain.* 2013;136(Pt 12):3578–88. <https://doi.org/10.1093/brain/awt287>.
26. Liu GY, Sabatini DM. mTOR at the nexus of nutrition, growth, ageing and disease. *Nat Rev Mol Cell Biol.* 2020;21(4):183–203. <https://doi.org/10.1038/s41580-019-0199-y>.
27. Liu P, Yang X, Hei C, Meli Y, Niu J, Sun T, Li PA. Rapamycin reduced ischemic brain damage in diabetic animals is associated with suppressions of mTOR and ERK1/2 signaling. *Int J Biol Sci.* 2016;12(8):1032–40. <https://doi.org/10.7150/ijbs.15624>.
28. Liu Y, Xue X, Zhang H, Che X, Luo J, Wang P, Xu J, Xing Z, Yuan L, Liu Y, Fu X, Su D, Sun S, Zhang H, Wu C, Yang J. Neuronal-targeted TFEB rescues dysfunction of the autophagy-lysosomal pathway and alleviates ischemic injury in permanent cerebral ischemia. *Autophagy.* 2019;15(3):493–509. <https://doi.org/10.1080/15548627.2018.1531196>.
29. Lu Y, Zhao Y, Zhang Q, Fang C, Bao A, Dong W, Peng Y, Peng H, Ju Z, He J, Zhang Y, Xu T, Zhong C. Soluble TREM2 is associated with death and cardiovascular events after acute ischemic stroke: an observational study from CATIS. *J Neuroinflammation.* 2022;19(1):88. <https://doi.org/10.1186/s12974-022-02440-y>.
30. Mansfield A, Inness EL, McIlroy WE. Stroke. *Handb Clin Neurol.* 2018;159:205–28. <https://doi.org/10.1016/b978-0-444-63916-5.00013-6>.
31. Masuda T, Croom D, Hida H, Kirov SA. Capillary blood flow around microglial somata determines dynamics of microglial processes in ischemic conditions. *Glia.* 2011;59(11):1744–53. <https://doi.org/10.1002/glia.21220>.
32. Mateos L, Perez-Alvarez MJ, Wandosell F. Angiotensin II type-2 receptor stimulation induces neuronal VEGF synthesis after cerebral ischemia. *Biochim Biophys Acta.* 2016;1862(7):1297–308. <https://doi.org/10.1016/j.bbadis.2016.03.013>.
33. McKeage K, Murdoch D, Goa KL. The sirolimus-eluting stent: a review of its use in the treatment of coronary artery disease. *Am J Cardiovasc Drugs.* 2003;3(3):211–30. <https://doi.org/10.2165/00129784-20030303-00007>.
34. Meschia JF, Brott T. Ischaemic stroke. *Eur J Neurol.* 2018;25(1):35–40. <https://doi.org/10.1111/ene.13409>.
35. Meyuhos O. Ribosomal protein S6 phosphorylation: four decades of research. *Int Rev Cell Mol Biol.* 2015;320:41–73. <https://doi.org/10.1016/bs.ircmb.2015.07.006>.
36. Moore EE, Liu D, Li J, Schimmel SJ, Cambronero FE, Terry JG, Nair S, Pechman KR, Moore ME, Bell SP, Beckman JA, Gifford KA, Hohman TJ, Blennow K, Zetterberg H, Carr JJ, Jefferson AL. Association of aortic stiffness with biomarkers of neuroinflammation, synaptic dysfunction, and neurodegeneration. *Neurology.* 2021;97(4):e329–40. <https://doi.org/10.1212/wnl.000000000012257>.
37. Morrison HW, Filosa JA. A quantitative spatiotemporal analysis of microglia morphology during ischemic stroke and reperfusion. *J Neuroinflammation.* 2013;10:4. <https://doi.org/10.1186/1742-2094-10-4>.
38. Orset C, Macrez R, Young AR, Panthou D, Angles-Cano E, Maubert E, Agin V, Vivien D. Mouse model of in situ thromboembolic stroke and reperfusion. *Stroke.* 2007;38(10):2771–8. <https://doi.org/10.1161/strokeaha.107.487520>.
39. Pan YW, Wu DP, Liang HF, Tang GY, Fan CL, Shi L, Ye WC, Li MM. Total saponins of panax notoginseng activate Akt/mTOR pathway and exhibit neuroprotection in vitro and in vivo against ischemic damage. *Chin J Integr Med.* 2022;28(5):410–8. <https://doi.org/10.1007/s11655-021-3454-y>.
40. Paolicelli RC, Sierra A, Stevens B, Tremblay ME, Aguzzi A, Ajami B, Amit I, Audinat E, Bechmann I, Bennett M, Bennett F, Bessis A, Biber K, Bilbo S, Blurton-Jones M, Boddeke E, Brites D, Bröne B, Brown GC, Wyss-Coray T. Microglia states and nomenclature: a field at its crossroads. *Neuron.* 2022;110(21):3458–83. <https://doi.org/10.1016/j.neuron.2022.10.020>.
41. Perez-Alvarez MJ, Mateos L, Alonso A, Wandosell F. Estradiol and progesterone administration after pMCAO stimulates the neurological recovery and reduces the detrimental effect of ischemia mainly in hippocampus. *Mol Neurobiol.* 2015;52(3):1690–703. <https://doi.org/10.1007/s12035-014-8963-7>.
42. Pérez-Álvarez MJ, Maza Mdel C, Anton M, Ordoñez L, Wandosell F. Post-ischemic estradiol treatment reduced glial response and triggers distinct cortical and hippocampal signaling in a rat model of cerebral ischemia. *J Neuroinflammation.* 2012;9:157. <https://doi.org/10.1186/1742-2094-9-157>.
43. Perez-Alvarez MJ, Villa Gonzalez M, Benito-Cuesta I, Wandosell FG. Role of mTORC1 controlling proteostasis after brain ischemia. *Front Neurosci.* 2018;12:60. <https://doi.org/10.3389/fnins.2018.00060>.
44. Perez-Alvarez MJ, Wandosell F. Stroke and neuroinflammation: role of sexual hormones. *Curr Pharm Des.* 2016;22(10):1334–49. <https://doi.org/10.2174/138161282210160304112834>.
45. Qin C, Zhou LQ, Ma XT, Hu ZW, Yang S, Chen M, Bosco DB, Wu LJ, Tian DS. Dual functions of microglia in ischemic stroke. *Neurosci Bull.* 2019;35(5):921–33. <https://doi.org/10.1007/s12264-019-00388-3>.
46. Rupalla K, Allegrini PR, Sauer D, Wiessner C. Time course of microglia activation and apoptosis in various brain regions after permanent focal cerebral ischemia in mice. *Acta Neuropathol.* 1998;96(2):172–8. <https://doi.org/10.1007/s004010050878>.



47. Sarbassov DD, Guertin DA, Ali SM, Sabatini DM. Phosphorylation and regulation of Akt/PKB by the rictor-mTOR complex. *Science*. 2005;307(5712):1098–101. <https://doi.org/10.1126/science.1106148>.
48. Simats A, Liesz A. Systemic inflammation after stroke: implications for post-stroke comorbidities. *EMBO Mol Med*. 2022;14(9):16269. <https://doi.org/10.15252/emmm.202216269>.
49. Sommer CJ. Ischemic stroke: experimental models and reality. *Acta Neuropathol*. 2017;133(2):245–61. <https://doi.org/10.1007/s00401-017-1667-0>.
50. Tewari D, Sah AN, Bawari S, Nabavi SF, Dehpour AR, Shirooie S, Braidly N, Fiebich BL, Vacca RA, Nabavi SM. Role of nitric oxide in neurodegeneration: function, regulation, and inhibition. *Curr Neuropharmacol*. 2021;19(2):114–26. <https://doi.org/10.2174/1570159x1866620042901549>.
51. Villa-González M, Martín-López G, Pérez-Álvarez MJ. Dysregulation of mTOR signaling after brain ischemia. *Int J Mol Sci*. 2022. <https://doi.org/10.3390/ijms23052814>.
52. Virani SS, Alonso A, Aparicio HJ, Benjamin EJ, Bittencourt MS, Callaway CW, Carson AP, Chamberlain AM, Cheng S, Delling FN, Elkind MSV, Evenson KR, Ferguson JF, Gupta DK, Khan SS, Kissela BM, Knutson KL, Lee CD, Lewis TT, Tsao CW. Heart disease and stroke statistics-2021 update: a report from the american heart association. *Circulation*. 2021;143(8):e254–743. <https://doi.org/10.1161/cir.0000000000000950>.
53. Wu M, Zhang H, Kai J, Zhu F, Dong J, Xu Z, Wong M, Zeng LH. Rapamycin prevents cerebral stroke by modulating apoptosis and autophagy in penumbra in rats. *Ann Clin Transl Neurol*. 2018;5(2):138–46. <https://doi.org/10.1002/acn3.507>.
54. Xia Q, Zhan G, Mao M, Zhao Y, Li X. TRIM45 causes neuronal damage by aggravating microglia-mediated neuroinflammation upon cerebral ischemia and reperfusion injury. *Exp Mol Med*. 2022;54(2):180–93. <https://doi.org/10.1038/s12276-022-00734-y>.
55. Yang X, Hei C, Liu P, Song Y, Thomas T, Tshimanga S, Wang F, Niu J, Sun T, Li PA. Inhibition of mTOR pathway by rapamycin reduces brain damage in rats subjected to transient forebrain ischemia. *Int J Biol Sci*. 2015;11(12):1424–35. <https://doi.org/10.7150/ijbs.12930>.
56. Zietz A, Gorey S, Kelly PJ, Katan M, McCabe J. Targeting inflammation to reduce recurrent stroke. *Int J Stroke*. 2023. <https://doi.org/10.1177/17474930231207777>.

## Publisher's Note

Springer Nature remains neutral with regard to jurisdictional claims in published maps and institutional affiliations.